

Diffraction Dissociation and the 1.40-GeV πN Peak in p - p Collisions

L. RESNICK*

The Niels Bohr Institute, Copenhagen, Denmark

(Received 26 May 1966)

The quasidiffraction model of Drell and Hiida is applied in an attempt to understand the 1.40-GeV maximum seen in high-energy, small-angle, inelastic p - p scattering. Reasonable agreement is found in absolute magnitude, and in dependence on the energy and scattering angle, but the correct position and width cannot be fitted quite accurately; several different phenomenological form factors are attempted. It is shown that, at very forward angles, there is a cancellation in dependence on the off-shell pion mass between the pion propagator and a kinematic factor arising from the diffraction scattering. This leads to a suppression of waves with angular momentum $j > \frac{1}{2}$ for the recoiling system, and might be an explanation for the prominence at very small angles of the 1.40-GeV bump relative to the d_{13} and f_{15} isobars.

I. INTRODUCTION

RECENT high-energy proton-proton scattering experiments at CERN¹ and Brookhaven² have shown an interesting structure in the inelastic spectrum. In addition to the bumps at 1.51 and 1.69 GeV, which had already been seen by Cocconi *et al.*³ and identified with the well-known d_{13} and $f_{15} \pi N$ isobars, a very prominent bump at 1.40 GeV is also seen at the smallest angles ($\lesssim 20$ mrad). (This bump and the one at 1.51 GeV are not clearly resolved as two distinct peaks²; rather, as the laboratory scattering angle θ is increased, the very large prominence at ≈ 1.40 GeV decreases in magnitude very quickly, and seems to shift toward larger mass values, until only a well-defined bump at ≈ 1.51 GeV remains, which can be identified with the d_{13} .) The 1.51- and 1.69-GeV bumps at the larger angles (40–60 mrad, for 15-GeV incoming energy) have a roughly similar dependence on θ . By contrast, the 1.40-GeV object is produced much more prominently at the smallest angles. For an incoming energy of 15 GeV, and $\theta = 10$ mrad, the magnitude of this bump is some 2.5 times as big as that of the 1.69-GeV bump; while already at 25 mrad, it is indistinguishable from background.

It has been suggested¹ that the 1.40-GeV peak is due to the $p_{11} \pi N$ interaction at ≈ 1400 MeV. Recent analyses^{4,5} have shown a rapidly rising phase shift in this region, possibly indicating a resonance; though the phase shift does not seem to reach 90° ,⁵ and the large inelasticity in the $p_{11} \pi N$ reaction makes the situation somewhat unclear. If there is indeed a $p_{11} \pi N$ resonance near 1.40 GeV, the corresponding bump in the inelastic spectrum could then be attributed to such a recoiling isobar, similar to the other two well-known isobars.

* Most of this work was done at Brookhaven National Laboratory, under the auspices of the U. S. Atomic Energy Commission.

¹ G. Bellettini *et al.*, Phys. Letters **18**, 167 (1965). There are further references here.

² G. B. Collins *et al.*, report submitted to the Oxford International Conference on Elementary Particles, September 1965. E. W. Anderson *et al.*, Phys. Rev. Letters **16**, 855 (1966).

³ G. Cocconi *et al.*, Phys. Rev. Letters **7**, 450 (1961).

⁴ L. D. Roper, Phys. Rev. Letters **12**, 340 (1964); L. D. Roper and R. M. Wright, Phys. Rev. **135**, B921 (1965); P. Auvil *et al.*, Phys. Letters **12**, 76 (1964).

⁵ B. H. Bransden *et al.*, Phys. Rev. **139**, B1565 (1965).

However, there remains the problem of the difference in behavior noted in the previous paragraph between such a p_{11} isobar and the two others. A quasidiffraction model has often been proposed for the structure of the high-energy, small-angle inelastic spectrum.⁶ The relative suppression of the production of the d_{13} and f_{15} isobars at very small momentum transfers is then explained qualitatively as a mismatch of angular momentum at the target vertex, due to the coherent nature of the forward diffraction scattering.^{1,7} However, it would be desirable to have a specific production mechanism which accounts for this automatically.

The main purpose of this paper is to point out that such a mechanism already exists, in the quasidiffraction model of Drell and Hiida (hereinafter DH).^{8,9} This point is discussed in Sec. 4. For the sake of notation and clarity in the other sections, the DH model is briefly derived in Sec. 2.

The quasidiffraction model has also been applied by various authors¹⁰ to other processes, in particular with respect to the question of whether the A_1 bump is a dynamical resonance, or is purely a kinematical effect of the diffraction. Two experimental groups¹¹ have concluded that, at incoming pion energies of 3.6 and 6 GeV, the A_1 bump in the π - p spectrum can be accounted for by the quasidiffraction model. It is therefore of interest to raise the same question in the present case of high-energy p - p scattering of whether the bump at

⁶ W. D. Walker and M. L. Good, Phys. Rev. **120**, 1857 (1960).

⁷ G. Cocconi, in *Proceedings of the 1962 International Conference on High-Energy Nuclear Physics at CERN*, edited by J. Prentki (CERN, Geneva, 1962), p. 883.

⁸ S. D. Drell and K. Hiida, Phys. Rev. Letters **7**, 199 (1961).

⁹ M. M. Islam, Phys. Rev. **131**, 2292 (1963); Y. Takada and M. Bando, Progr. Theoret. Phys. (Kyoto) **33**, 657 (1965). These authors, as well as Drell and Hiida, apply the DH model only at larger θ and $|t|$, where only the d_{13} and f_{15} resonances are seen. Islam also performs partial-wave projections, and attempts to account for final-state interactions. But his calculations shed no special light on the region of very small θ ($|t| \lesssim 0.1$ GeV²), and are not concerned with the main point we wish to make in Sec. 4.

¹⁰ R. T. Deck, Phys. Rev. Letters **13**, 169 (1964); U. Maor and T. A. O'Halloran, Jr., Phys. Letters **15**, 281 (1965). These authors apply the diffraction model to the reaction $\pi + p \rightarrow \rho + \pi + p$. The kinematics are such that here the diffraction occurs at the lower vertex (in our terminology); what contributes is essentially the exchange graph of Fig. 1.

¹¹ B. C. Shen *et al.*, Phys. Rev. Letters **15**, 731 (1965); V. E. Barnes *et al.*, *ibid.* **16**, 41 (1966).

1.40 GeV might not perhaps be already accounted for by the kinematics of the DH process. This is precisely what Drell and Hiida attempted to do originally; but they examined energies of 16 and 25 GeV, and angles of 40 and 56 mrad, where the bump comes in the range 1.55 GeV to 1.70 GeV; and we now know that in this region there are two bumps, at 1.51 and 1.69 GeV, and readily attribute these to recoiling isobars. On the other hand, we are interested here in much smaller angles (0–15 mrad), where the DH peak occurs at ≈ 1.40 to ≈ 1.45 GeV. This is discussed in Sec. 3.

2. THE DH MODEL

Figure 1 is the diagram for the DH model. q, q' are the four-momenta, respectively, of the initial fast proton, and the scattered proton. p, p' are the target, and recoil protons; k' is the produced pion. q, p will also stand for the magnitudes of the corresponding three-momenta, $t \equiv (q - q')^2$ is the invariant momentum transfer in the diffracting system; $\Delta^2 \equiv (p - p')^2$ is the invariant mass squared of the virtual pion. $W^2 \equiv (k' + p')^2$, so that W is the energy of the recoiling k', p' system, and is the "missing mass" in the experiments. All symbols with superscript W indicate the corresponding quantity evaluated in the W center-of-mass system; the latter is defined by $\mathbf{k}'^W + \mathbf{p}'^W = 0$. Quantities without superscripts are evaluated in the laboratory system $\mathbf{p} = 0$. θ is the (laboratory) angle between the directions of q' and q . The metric is such that $\Delta^2, t^2 < 0$.

Let the invariant amplitude M be defined by

$$S = 1 - i(2\pi)^4 \delta^4(\sum_i p_i) [(2m)^4 / \prod_i (2E_{p_i})]^{1/2} M.$$

Then the doubly differential cross section $\delta\sigma \equiv d^2\sigma / d\Omega_{q'} d\Omega_{k'}$ is

$$\delta\sigma = \frac{m^3}{2(2\pi)^5} \frac{q'^2 k'^W}{q E_{q'} W} \frac{1}{4} \sum_{\text{spins}} \int d\Omega_{k'}^W |M|^2.$$

The invariant mass squared of the diffracting system is $s \equiv (q' + k')^2$, and the corresponding center-of-mass momentum, for a physical system, is

$$k \equiv [s - (m + \mu)^2]^{1/2} [s - (m - \mu)^2]^{1/2} / 2\sqrt{s}.$$

The model takes for M

$$M = M_a(s, t) \frac{G_r}{\mu^2 - \Delta^2} \bar{u}(p') \gamma_5 u(p), \quad (1)$$

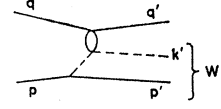
where M_a is the invariant amplitude for the diffraction scattering, and sets further

$$\frac{1}{2} \sum_{\text{spins}} |M_a|^2 = \left(\frac{4\pi\sqrt{s}}{m} \right)^2 \frac{d\sigma_a(s, t)}{d\Omega} \quad (2)$$

with σ_a the physical diffraction cross section. Now

$$d\sigma_a(s, t) / d\Omega = [d\sigma_a(s, 0) / d\Omega] g(t),$$

FIG. 1. The DH model. Further notation and definitions appear in the text.



where $g(t)$ is the shape of the physical diffraction peak, and is independent of s .¹² Under the assumption of a pure imaginary elastic amplitude, and using the optical theorem, we obtain

$$d\sigma_a(s, 0) / d\Omega = [(k/4\pi)\sigma_{\text{tot}}(s)]^2.$$

Also, $\sigma_{\text{tot}}(s)$ will be given its asymptotic value, and taken independent of s . With

$$\frac{1}{2} \sum_{\text{spins}} |\bar{u}(p') \gamma_5 u(p)|^2 = -\Delta^2 / 4m^2,$$

finally, we have

$$\delta\sigma = \frac{G_r^2}{8(2\pi)^5} \frac{g(t)\sigma_{\text{tot}}^2}{m} \frac{q'^2 k'^W}{q E_{q'} W} \int d\Omega_{k'}^W s k^2 (-\Delta^2)(\mu^2 - \Delta^2)^{-2}. \quad (3)$$

Neglecting the pion mass μ in $s k^2$, this factor simplifies to $\frac{1}{4}(s - m^2)^2$. If the polar axis is chosen along \mathbf{p}^W , Δ^2 is independent of the azimuthal angle ϕ^W . The integration

$$\frac{1}{8\pi} \int_0^{2\pi} d\phi^W (s - m^2)^2 \equiv h$$

can then be explicitly performed:

$$h = (E_{q'}^W E_{k'}^W + q'^W k'^W \cos\chi^W \cos\theta_{k'}^W)^2 + \frac{1}{2} (q'^W k'^W \sin\chi^W \sin\theta_{k'}^W)^2,$$

$$\cos\chi^W = [E_p^W (E_{q'}^W + W) - \frac{1}{2}(m^2 + W^2 + 2W E_{q'}^W)] / p^W q'^W. \quad (4)$$

The final W system can be $p\pi^0$, or $n\pi^+$; this gives a factor 3 in Eq. (3). However, the diffraction scattering at the upper vertex is a scalar process, mediated by a "vacuum-like" exchange. This is in accord with the idea of coherent forward scattering. This has already been implicitly assumed above by replacing the diffraction vertex by the scalar function $(s^{1/2}k/m)[g(t)]^{1/2}\sigma_{\text{tot}}$. Since no isospin exchange is allowed,¹³ the isospin of the W system must remain that of the target proton, $T = \frac{1}{2}$. A form factor $F(\Delta^2)$ is also introduced to account for off-shell effects. This is discussed further below. So $\delta\sigma$ becomes $(q'/E_{q'} \approx 1)$

$$\delta\sigma = \frac{9G_r^2}{24(2\pi)^4} \frac{g(t)\sigma_{\text{tot}}^2}{m} \frac{q'}{q} \frac{k'^W}{W} \int_{-1}^1 d(\cos\theta_{k'}^W) \times h(-\Delta^2)(\mu^2 - \Delta^2)^{-2} F(\Delta^2). \quad (5)$$

¹² That this is a reasonable procedure has been confirmed in the bubble-chamber experiments of Shen *et al.*, Ref. 11.

¹³ This argument for only $T=0$ exchange, leading to a suppression at high energy for all recoiling systems of $T \neq \frac{1}{2}$, was originally put forward by A. P. Contogouris, S. C. Frautschi, and H. Wong, Phys. Rev. **129**, 974 (1963).

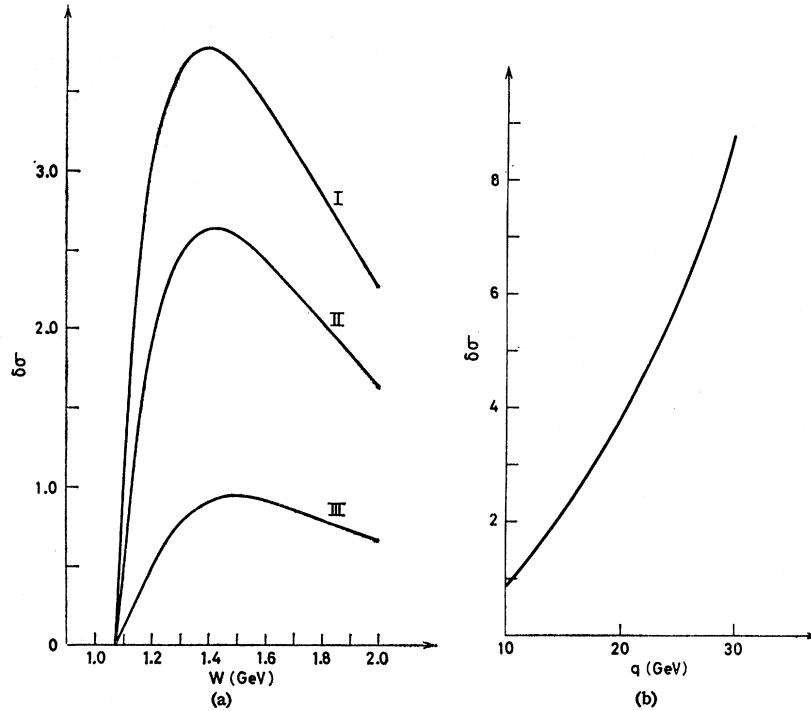


FIG. 2. (a) Plot of Eq. (6) with $F(\Delta^2) \equiv 1$, incoming momentum $q = 20$ GeV. I: $\theta = 0$. II: $\theta = 10$ mrad. III: $\theta = 20$ mrad. The ordinate scale here and in succeeding graphs is in b/sr GeV. (b) Plot of Eq. (6) with $F(\Delta^2) \equiv 1$, as a function of q , for the fixed values $\theta = 0$, $W = 1.40$ GeV.

Using

$$d(\cos\theta_{k'})^W = \frac{1}{2p^W p'^W} d(-\Delta^2) = \frac{W}{2mKk'^W} d(-\Delta^2),$$

($\mathbf{K} = \mathbf{p}' + \mathbf{k}'$, $K = |\mathbf{K}|$), this can also be written

$$\delta\sigma = \frac{9}{24(2\pi)^3} \frac{G_r^2}{4\pi} \frac{g(t)\sigma_{\text{tot}}^2}{m^2} \frac{q'}{q} \frac{1}{K} \int_A^B d(-\Delta^2) \times (-\Delta^2)(\mu^2 - \Delta^2)^{-2} h F(\Delta^2);$$

$$A = 2(E_p^W E_{p'}^W - m^2 - p^W k'^W),$$

$$B = 2(E_p^W E_{p'}^W - m^2 + p^W k'^W). \quad (6)$$

This is the formula given by DH.⁸

The following numerical values will be used in the subsequent calculations. $G_r^2/4\pi = 14.4$, $\sigma_{\text{tot}} = 28$ mb, $g(t) = \exp(9t + 2.5t^2)$.¹⁴ The conversion of the right-hand side (with all momenta in GeV) to b/sr GeV requires a further factor 2.55×10^{-3} .

3. SOME NUMERICAL RESULTS

Figure 2 shows $\delta\sigma$, given by formula (6) and with $F(\Delta^2)$ set equal to 1, for several values of q and θ . The following features can be noted: (i) The angular distribution is very sharply peaked toward small θ . This is guaranteed by the πp diffraction factor $g(t)$, and is a basic feature of the DH model. (ii) The cross section at $\theta = 0$ increases quadratically with q . This is to be sharply contrasted with a simple one-pion-exchange

¹⁴ K. J. Foley *et al.*, Phys. Rev. Letters 11, 425 (1963); 15, 45 (1965).

(O.P.E.) model with recoiling isobar, which is well known to be constant with q

$$(d^2\sigma/d\Omega dq' \sim q^2 \times d^2\sigma/dtdq' \sim q^2 \times q^{-2}).$$

Furthermore, this latter model, at $q = 20$ GeV and $\theta = 5$ mrad, gives a contribution ≈ 0.028 b/sr GeV (this last estimate is obtained for a recoiling p_{11} isobar which resonates at $W = 1.40$ GeV with no inelasticity); while formula (6) with $F = 1$ gives 3.26 b/sr GeV, which is somewhat larger than the experimental value of ≈ 1.5 b/sr GeV. Close agreement is not to be expected because of the effects of $F(\Delta^2)$ and of possible final-state interactions; this is discussed further below. However, this rough agreement in absolute magnitude of the cross section is gratifying; there were no free parameters available. (iii) The width of the peak in Fig. 2(a) is much too large to fit the experimental bump; this latter at $q = 20$ GeV has a full width Γ of ≈ 0.18 GeV, while the maximum that (6) generates is very much flatter. Therefore the simple form (6) with $F = 1$ is inadequate to fit the experimental data.

At this point, one may consider the influence of possible off-shell effects. After all, (6) with $F \equiv 1$ is the contribution of Fig. 1 at the pion pole $\Delta^2 = \mu^2$, while the range of Δ^2 that contributes is such that $\Delta^2 \ll -\mu^2$ ($B = 29\mu^2$ for $q = 20$ GeV, $\theta = 0$, $W = 1.4$ GeV). It is reasonable to introduce the form factor $F(\Delta^2)$ in the integrand of (5) or (6) to account for deviations from the perturbation theory expression. Unfortunately, this F is essentially unknown, so that a degree of arbitrariness is necessarily introduced. [It must be remembered, though, that the choice $F(\Delta^2) = 1$ is already an

arbitrary choice, and almost certainly wrong.] However, since F is constrained by $F(\mu^2)=1$, and the cross section is to be fitted in absolute magnitude as a function of W , for various q and θ , the model is still a meaningful and, possibly, a useful one.

We have tried sharp cutoffs at $-50\mu^2$, $-30\mu^2$, $-20\mu^2$, and exponential and Gaussian shapes. Figure 3 shows some of the results. It is seen that for very small θ , where $A \approx 0$ independently of W , the effect of the suppression of large $|\Delta^2|$ is also to suppress large W . For larger θ , A is already larger, and also increases with W , so F is less effective in sharpening the peak than it is in suppressing the whole curve altogether. However, at small θ , besides sharpening the peak, F also shifts the position to smaller values of W . For $q=20$ GeV and $\theta=10$ mrad, a sharp cutoff at $20\mu^2$ shifts the peak to $W=1.28$ GeV; the smoother cutoffs act similarly. An F which falls with $|\Delta^2|$ cannot narrow the calculated peak on the low- W side of the maximum, where also the experimental bump is sharper.

While the possibility that some choice of F exists which would give a narrow enough peak at the correct position has not been eliminated, we feel that this is unlikely in view of the cases actually tried. A steeply falling F seems to be necessary to suppress the high- W region appreciably; to narrow it down sufficiently, it seems unavoidable to also shift the position of the peak to too low values. We thus conclude that the DH model (6) is insufficient to account completely for the observed bump at 1.40 GeV; the correct position and width cannot quite be fitted at the same time.

4. PARTIAL-WAVE ANALYSIS

To consider the possible effects of final-state interactions between the slow nucleon and pion (we ignore here any interaction between the fast proton and the other particles, except for the diffraction scattering which has already been accounted for), it is necessary to analyze the amplitude into the different partial waves

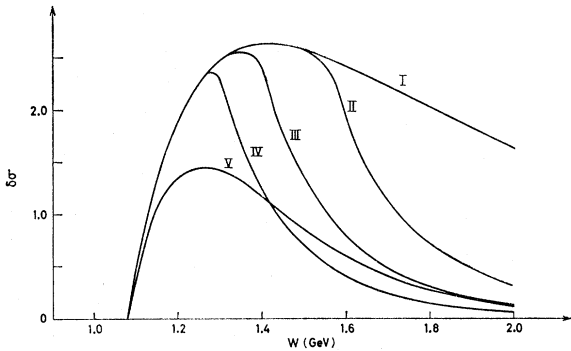


FIG. 3. Equation (6), as a function of W , for fixed $q=20$ GeV, $\theta=10$ mrad, and various $F(\Delta^2)$. I: $F=1$. II: $F=\bar{\theta}(\Delta^2+50\mu^2)$, where $\bar{\theta}$ =the step function. III: $F=\bar{\theta}(\Delta^2+30\mu^2)$. IV: $F=\bar{\theta}(\Delta^2+20\mu^2)$. V: $F=\exp[-2.21(\mu^2-\Delta^2)]$. This function = 0.5 at $\Delta^2=-15\mu^2$.

of the W system. We examine this partial-wave analysis in this section; the actual inclusion of final-state effects is not attempted in the present paper.

At this point, the assumption mentioned earlier in Sec. 2, that M has the form (1) with $M_a \sim (d\sigma_a/d\Omega)^{1/2}$ and independent of the spins of q and q' , is vital. The effective amplitude leading to the final $(\pi N)W$ system is then of the nature "scalar object" + nucleon \rightarrow pion + nucleon, where "scalar object" is the effective bubble at the diffracting $\pi\pi$ vertex. The projection of angular momentum j , parity $(-1)^{j\pm 1/2}$ (denoted $j\pm$), is then proportional to $I_{j\pm}$.

$$I_{j\pm} = \int_{-1}^1 dz [J_+ J_- P_{j\pm\frac{1}{2}}(z) - J_- J_+ P_{j\mp\frac{1}{2}}(z)] \times \frac{\bar{h}(z)}{\mu^2 - \Delta^2} [F(\Delta^2)]^{1/2},$$

$$z = \cos\theta_{k'}^W,$$

$$J_{\pm} = (E_p^W \pm m)^{1/2}, \quad J_{\pm}' = (E_{p'}^W \pm m)^{1/2},$$

$$\bar{h}(z) = \frac{1}{4\pi} \int_0^{2\pi} d\phi^W (s - m^2)$$

$$= E_{q'}^W E_{k'}^W + q'^W k'^W \cos\chi^W z. \quad (7)$$

The corresponding contribution to the cross section is

$$\delta\sigma_{j\pm} = \frac{9}{24(2\pi)^3} \frac{G_r^2}{4\pi} \frac{g(t)\sigma_{\text{tot}}^2}{m} \frac{q'}{q} \frac{k'^W}{W} (j + \frac{1}{2}) |I_{j\pm}|^2. \quad (8)$$

From (7) and (8) it is clear that, if $\bar{h}(\mu^2 - \Delta^2)^{-1}$ is independent of z and F is set = 1, there is no contribution to $\delta\sigma$ except for $j = \frac{1}{2}$, i.e., for s_{11} and p_{11} waves. That at $\theta=0$, the dependence on $\cos\theta_{k'}^W$ of \bar{h} and $\mu^2 - \Delta^2$ cancel to a remarkable degree we now proceed to show.

First, we note a qualitative argument. At $\theta=0$, the momenta \mathbf{q} , \mathbf{q}' , and \mathbf{K} are parallel. A Lorentz transformation to the W c.m. system leaves \mathbf{q}^W and \mathbf{q}'^W still parallel in the original direction, with \mathbf{p}^W antiparallel. In this system, since $\mathbf{p}'^W = -\mathbf{k}'^W$, and ϕ^W is degenerate, one can readily convince oneself that $s(z)$ and $\Delta^2(z)$ are large or small simultaneously, so that there is effective cancellation. Though each factor separately has a huge variation with z [at $q=20$ GeV, $W=1.40$ GeV, $\mu^2 - \Delta^2$ goes from μ^2 to $30\mu^2$ in the range $-1 \leq z \leq 1$; this is a factor 30 in the amplitude, or 900 in the expression (5) for the cross section], we now show quantitatively that the cancellation is almost exact. At $\theta=0$, $\chi^W = \pi$ and $\bar{h} = q' \cdot k'$. Also, for $|\mathbf{q}|$ large and $\theta=0$, $t \approx 0$ ($|t| \ll \mu^2$), while $k' \cdot (q' - q) \approx -k' \cdot q' \epsilon / |\mathbf{q}'|$, where

$$\epsilon = E_q - E_{q'} \approx |\mathbf{q}| - |\mathbf{q}'|.$$

Then, since

$$\Delta^2 = (q' + k' - q)^2 = t + \mu^2 + 2k' \cdot (q' - q),$$

we have $k' \cdot q' (\mu^2 - \Delta^2)^{-1} \approx |\mathbf{q}'| / 2\epsilon = \text{large constant}$. This holds only at $\theta=0$, and within the approximations made [DH model, neglect of terms $\sim \mu^2$ and $(m/q)^2$ effects].

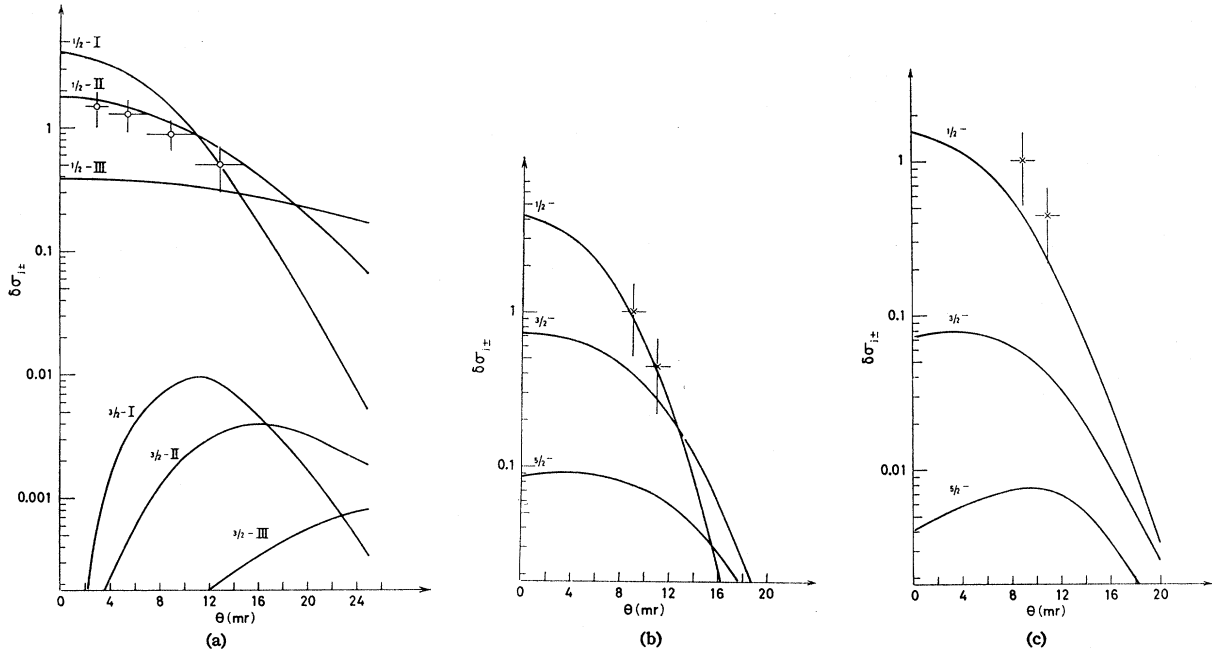


FIG. 4. (a) Equation (8), as a function of θ , for $\sqrt{F} \equiv 1$. The curves labeled I, II, III are, respectively, at incoming momenta $q = 30, 20, 10$ GeV. Here, and in (b) and (c), $1/2^-$ refers to p_{11} and is evaluated for $W = 1.40$ GeV; $3/2^-$ is d_{13} , and is evaluated for $W = 1.51$ GeV; $5/2^-$ is f_{15} , and is evaluated at $W = 1.69$ GeV. The circles are experimental points at $q = 20$ GeV, taken from Ref. 1. (b) Equation (8), as a function of θ , for fixed $q = 30$ GeV, and $\sqrt{F} = \bar{\theta}(\Delta^2 + 30\mu^2)$. This corresponds to a sharp cutoff in the cross section at $-15\mu^2$. The crosses are experimental points at 30 GeV from Ref. 2. (c) Same as (b) except $\sqrt{F} = \exp[-1.275(\mu^2 - \Delta^2)]$, $\sqrt{F} = \sqrt{0.5}$ at $\Delta^2 \approx -13\mu^2$.

Thus, at $\theta = 0$ and with $F = 1$, $\delta\sigma_{3/2^-} = \delta\sigma_{5/2^-} = 0$ in this model; for $\theta \neq 0$ and/or $F(\Delta^2) \neq \text{constant}$, this is no longer true. But for reasonably behaved $F(\Delta^2)$, a strong suppression of the contribution from angular momentum $> \frac{1}{2}$ at very small angles can still be expected.

Figure 4 shows some numerical calculations for various partial waves, and choice of F , bearing this out. Gaussian-shaped F , which were also tried, gave similar results, usually between the sharp cutoff and exponential cases. A few experimental points have also been included; these were obtained by subtracting a smooth background from the experimental peak, a procedure with very large inherent errors. There is rough agreement in absolute magnitude between the points and the p_{11} partial wave. On the other hand, there is an approximately equal s_{11} contribution which has not been plotted; including it would essentially double the calculated p_{11} curves. Considering the experimental errors due to the ambiguity of the background (and possibly the overlap with the 1.51-GeV bump), and the problem of final-state interactions in the s_{11} and p_{11} states, a more accurate comparison does not seem feasible at present.

5. CONCLUDING REMARKS

We first summarize briefly. In contrast with the small contribution from the model of O.P.E. with recoiling isobar, the DH model was seen to give a large effect at large energies and small angles, in rough agreement with

the magnitude seen experimentally. At a fixed large energy, it decreases very rapidly with θ , at least as fast as the π - p diffraction scattering [or faster, depending on $F(\Delta^2)$]. Again, this agrees with the experimental situation, where the observed bump seems to decrease at least as fast as the p - p elastic diffraction scattering.¹⁵ Though the position of the DH peak shifts to larger W with increasing q and θ , the shift is very small for $10 \text{ GeV} < q < 30 \text{ GeV}$, $0 < \theta < 15 \text{ mrad}$; the position is roughly between $W = 1.35$ GeV and $W = 1.45$ GeV in this region (with $F = 1$). This is close to the values for the observed bump.

All this makes the DH model an attractive candidate for the main production mechanism of the observed bump. However, as seen in Sec. 3, it is not able to satisfactorily account for the detailed position and width. The latter is therefore quite likely to be due also to a final-state interaction of the $(\pi N) W$ system. The contributions to s_{11} and p_{11} are roughly equal in the range $1.30 \text{ GeV} < W < 2.0 \text{ GeV}$. However, the s_{11} phase shift is still small at ≈ 1.40 GeV; it might be rising rapidly near 1.53 GeV.⁵ But there, the DH contribution is already smaller for any reasonable $F(\Delta^2)$. Nevertheless, such an s_{11} interaction might make a non-negligible

¹⁵ $\delta\sigma$, for fixed t , is very nearly quadratic in q , so $d\sigma/dt$ is essentially constant in this model, in agreement with experiment. For fixed q , Ref. 2 indicates $d\sigma \propto \exp(18t)$ on averaging over q values; while $\exp(18t)$ fits the $\frac{1}{2}^-$ curve of Fig. 4(c) excellently for $0 < \theta < 15 \text{ mrad}$. Thus, with this $F(\Delta^2)$, the behavior of $g(t) \approx \exp(9t)$ is effectively steepened to $\exp(18t)$, in very good agreement with experiment.

contribution, and this effect should also be examined. Such final-state interaction effects have not yet been included in these calculations, because these s_{11} and p_{11} interactions are highly inelastic, leading to a rather complicated analysis. We hope to deal with this problem separately later.

There are other open questions with regard to the model. An important one is the possible contribution of other graphs. Figure 5, the exchange graph to Fig. 1, is not important because of the kinematics of the experiments which select a high-energy final proton, so the pion is low energy, and the diffraction scattering cannot occur at the lower vertex. However, many other graphs are certainly possible. In particular, Fig. 6 shows two such possibilities; here, the incoming proton diffraction scatters off the target proton, with pion emission either before or after. This scattering off the core of the target, instead of off the pion in the cloud, should certainly be considered. We have examined Fig. 6(b). Here, of necessity, the final πN system must be p_{11} . Assuming scalar diffraction, as before, and relating it to $\sigma_{tot}^{\pi N}$ now instead of $\sigma_{tot}^{\pi p}$, Fig. 6(b) gives a contribution at $q=20$ GeV, $\theta=10$ mrad, larger than and very similar in shape to that in Fig. 2(a), i.e., the contribution from Fig. 1, with $F(\Delta^2)=1$. Here, however, the proton is off shell and it is harder to find a mechanism that would narrow the very wide peak. Perhaps such nucleon pole graphs contribute to the background. The importance of these and other graphs (such as successive diffraction scatterings) is at present not known. We do not consider this further here, the philosophy for now being to concentrate on Fig. 1 alone, and to calculate its contributions.

The question of final-state interactions sharpens the significance of Sec. 4, which is perhaps the main part of this paper. If the structure of the inelastic p - p spectrum is in fact due mainly to recoiling isobars, it is hard to understand *a priori* the difference in the behavior of the 1.40-GeV bump from the others, except by invoking general arguments about the coherence of forward

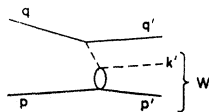


FIG. 5. The exchange graph to Fig. 1. For $E_q - E_{q'} \lesssim 1$ GeV, the pion k' has low energy, so the bubble corresponds to $\pi N \rightarrow \pi N$ scattering at $W \approx 1.4$ GeV, rather than diffraction scattering. This is essentially the graph for the isobar model, briefly discussed in Sec. 3.

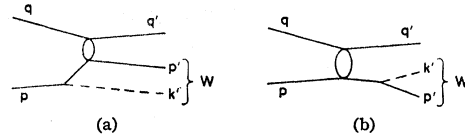


FIG. 6. (a) Diffraction scattering off the proton, with initial-state pion emission. If Fig. 1 corresponds to a “*t* channel” pion pole, this graph corresponds to a “*u* channel” nucleon pole. (b) Diffraction scattering off the proton, with final-state pion emission. This would correspond to a direct “*s*-channel” nucleon pole.

diffraction scattering. But the process is in fact inelastic, and the coherence is to be between the initial proton and the final isobar of mass 1.40 GeV, a 50% increase in mass; and both particles are physical. It is not clear that arguments of coherence giving selection rules of $\Delta j=0$ are very convincing under these circumstances. What was shown in Sec. 4 was that a specific model for how such quasidiffraction scattering might proceed exists; and that this model leads in a natural way to the selection rule $\Delta j=0$ (or at least $\Delta j \neq 0$ is strongly suppressed). In this DH model, the coherent diffraction scattering is for *virtual* $\pi + N \rightarrow \pi + N$. Insofar as the change of the mass of the pion is neglected by setting $F=1$, the rule $\Delta j=0$ is exact. But allowing for $F \neq 1$ shows that *some* $\Delta j \neq 0$ contribution is allowed at $\theta=0$. It is also interesting to note that a change in *parity* is allowed (proton $\rightarrow s_{11}$); this is contrary to the predictions based only on coherence, which do not allow the change of any quantum numbers.

The model discussed can account, in a semiquantitative way, for many of the known experimental facts about the 1.40-GeV bump. A more careful quantitative comparison must await further calculations including final-state effects; in these calculations, $F(\Delta^2)$ will be a (largely) undetermined function. But the results must then carefully fit experiment for different q, θ, W . This should be a severe test for the correctness of the model.

ACKNOWLEDGMENTS

I wish to thank the National Research Council of Canada for an overseas fellowship, and Professor Aage Bohr for the hospitality of the Niels Bohr Institute, where this was written.

I am grateful to Dr. R. F. Peierls, Dr. F. Selleri, and Dr. J. Hamilton for some very informative conversations. Special thanks are due Dr. F. Turkot for interesting me in the problem, and to him and the Brookhaven group for much experimental information.